JACS
JOURNAL OF THE AMERICAN CHEMICAL SOCIETY
Article
pubs.acs.org/JACS

Quasi-Racemic X-ray Structures of K27-Linked Ubiquitin Chains Prepared by Total Chemical Synthesis

Man Pan,[†,#] Shuai Gao,[†,#] Yong Zheng,[†,#] Xiaodan Tan,[†] Huan Lan,[†] Xianglong Tan,[†] Demeng Sun,[†] Lining Lu,[†] Tian Wang,[†] Qingyun Zheng,[†] Yichao Huang,[†] Jiawei Wang,[‡] and Lei Liu*[,†]

[†]Tsinghua-Peking Center for Life Sciences, Ministry of Education Key Laboratory of Bioorganic Phosphorus Chemistry and Chemical Biology, Department of Chemistry, Tsinghua University, Beijing 100084, China

[‡]State Key Laboratory of Biomembrane and Membrane Biotechnology, Center for Structural Biology, School of Life Sciences, Tsinghua University, Beijing 100084, China

Supporting Information

ABSTRACT: Quasi-racemic crystallography has been used to determine the X-ray structures of K27-linked ubiquitin (Ub) chains prepared through total chemical synthesis. Crystal structures of K27-linked di- and tri-ubiquitins reveal that the isopeptide linkages are confined in a unique buried conformation, which provides the molecular basis for the distinctive function of K27 linkage compared to the other seven Ub chains. K27-linked di- and triUb were found to adopt different structural conformations in the crystals, one being symmetric whereas the other triangular. Furthermore, bioactivity experiments showed that the ovarian tumor family de-ubiquitinase 2 significantly favors K27-linked triUb than K27-linked diUb. K27-linked triUb represents the so-far largest chemically synthesized protein (228 amino acids) that has been crystallized to afford a high-resolution X-ray structure.

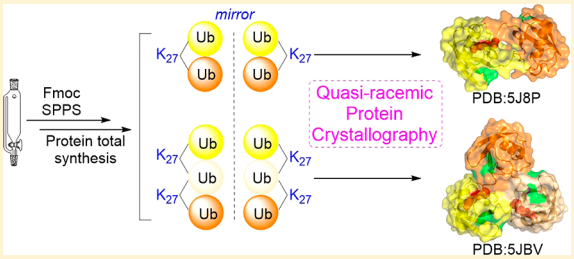

INTRODUCTION

Protein ubiquitination is a prevalent post-translational modification in many cellular processes such as protein degradation, autophagy, DNA repair, cell signaling and immune response.[1−3] This modification is controlled by a cascade of enzymes (E1, E2, and E3) that install the C-terminus of 76-amino-acid ubiquitin (Ub) onto the substrate lysine to afford an isopeptide bond.[4−6] There are eight types of Ub chains, containing covalent linkages of a donor Ub anchored to lysines (K6, K11, K27, K29, K33, K48, and K63) or N-terminus (M1) of an acceptor Ub.[2,7,8] The different linkage Ub's can be recognized by chain-specific binder proteins leading to distinct biological functions.[2,9,10]

To elucidate the molecular mechanisms of Ub's, studies have been performed to solve crystal structures of di-, tri-, and tetraUb chains. K6-,[11] K11-,[12,13] and K48-linked diUb's[14] favor compact structures where Ub units bind each other through extensive hydrophobic interactions. In contrast, linear and K63-linked diUb's adopt open conformations with less contact between Ub units.[15] More recent studies on the structures of K29 and K33-linked Ub's reveal distinctive flexible conformations.[16−18] Nonetheless, no crystal structure has been reported for K27-linked Ub's.

K27-linked Ub's were initially identified in the cellar process of lysosomal localization[19] and mitochondrial autophagy.[20] More recently they were found to play important roles in autoimmunity[21] and DNA damage response.[22] To investigate these interesting functions, it is crucial to carry out biochemical and structural studies of K27-linked Ub's. However, enzymatic reconstitution of K27-linked Ub chains has remained elusive.[23,24]

Using the technology of genetically encoded orthogonal protection and activated ligation,[11,25] Fushman et al. prepared K27-linked diUb and examined its nuclear magnetic resonance (NMR) structure. Compared to the diUb's of other linkages, K27-linked diUb exhibits unique NMR characteristics and resistance to cleavage by de-ubiquitinases (DUBs).[26,27] To further elucidate the structural features of K27-linked Ub's, we now report the total chemical synthesis of K27-linked di- and triUb's in both L- and D-protein forms. Using the technology of quasi-racemic crystallography, we obtained the X-ray structures of K27-linked di- (resolution 1.6 Å) and triUb's (resolution 2.1 Å) for the first time.

RESULTS AND DISCUSSION

Total Synthesis and Structure Determination of K27-Linked diUb. Our total synthesis employed the strategy of hydrazide-based native chemical ligation[28−31] and microwave-assisted solid phase peptide synthesis (SPPS)[32,33] (Figure 1A,B). A trifluoroacetic acid (TFA)-labile 1-(2,4-dimethoxyphenyl)-2-mercaptoethyl auxiliary (Aux) was employed to enable the construction of the isopeptide bond.[34,35] The K27-linked diUb containing 152 amino acids (aa) was divided into four peptide segments, namely Ub[Cys(Acm)$_{46}$-Gly$_{75}$]-NHNH$_2$ (**1**), Ub[Met$_1$-Lys(Aux-Gly)$_{27}$-Phe$_{45}$]-NHNH$_2$ (**2**),

Received: April 19, 2016
Published: June 6, 2016

DOI: 10.1021/jacs.6b04031
J. Am. Chem. Soc. 2016, 138, 7429−7435

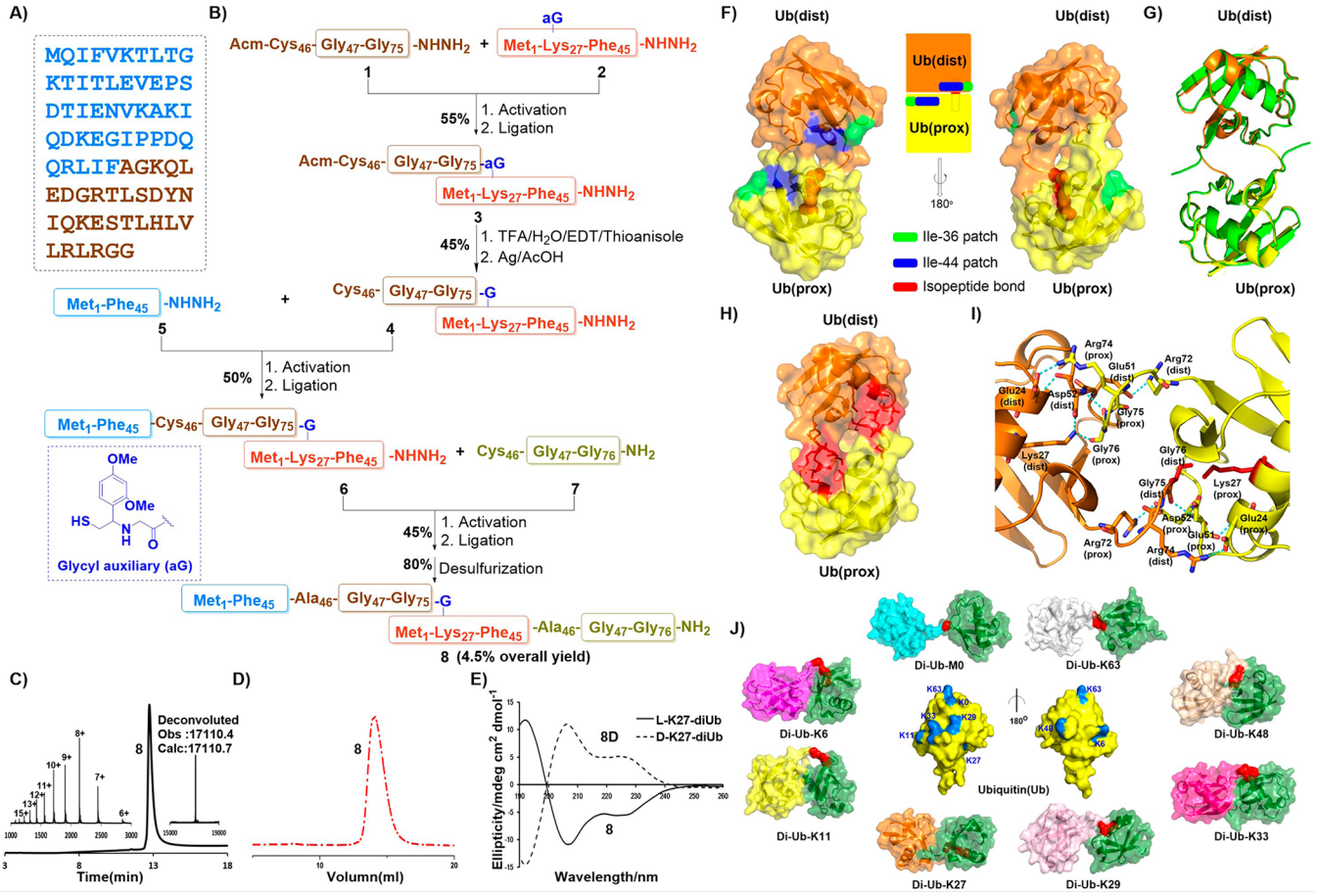

Figure 1. K27-linked diUb. (A) Amino acid sequence of Ub. (B) Synthetic route. (C) Analytical HPLC chromatogram (λ = 214 nm) of isolated product **8**. Inset: Observed ESI-MS of the main peak and deconvoluted electrospray ionization mass spectrum of **8** (observed mass = 17 111.2 Da, calculated mass = 17 110.7 Da, average isotopes). (D) Gel filtration chromatography (λ = 280 nm, Superdex 75 column (10/300 GL)) of **8**. (E) Circular dichroism spectra of L- and D-forms (Figure S3) of K27-linked diUb. (F) Schematic drawing of K27-linked diUb (center) and two views of K27-linked diUb crystal structure (left and right), with the distal Ub (orange), the proximal Ub (yellow) and the inside isopeptide bonds showed in spheres (red). (G) The alignment of monoUb colored in green with both Ub units in K27-linked diUb. (H) The interface (red) between distal Ub and proximal Ub. (I) Close-up view of the K27-linked diUb dimer interface. Residues shown in stick representation, distal interface (orange), and for the proximal interface (yellow). These polar interactions (<3.5 Å) are connected with dotted lines (cyan), and the isopeptide bond of Gly76dist and Lys27prox are drawn in red sticks. (J) Structures of all eight linkage diUb's: K27 (PDB: 5J8P), K6 (PDB: 2XK5), K11 (PDB: 2XEW, as representative), K29 (PDB: 4S22), K33 (PDB: 4XYZ), K48 (PDB: 3M3J, as representative), K63 (PDB: 2JF5, as representative), and diUb and linear diUb (PDB: 2W9N, as representative). At the center is monoUb (PDB: 1UBQ) in yellow surface representation. Acceptor Ub is colored in forest green, and donor Ub's are colored in different colors. Isopeptide bonds are shown in sphere representation (red).

Ub[Met_1-Phe_{45}]-$NHNH_2$ (**5**) and Ub[Cys_{46}-Gly_{76}] (**7**). Ala46 of each Ub unit was temporarily mutated to Cys as the ligation site. Gly76 of the distal Ub was incorporated to **2** through the building block glycyl auxiliary. An acetamidomethyl (Acm) group was used to protect the thiol group of N-terminal Cys of segment **1** to avoid oligomerization or self-cyclization.

The synthesis started with ligation of **1** and **2** to produce **3** with the specific Lys27-linked isopeptide bond. The Acm and Aux groups were then removed to afford **4**. After two more steps of ligation reactions, desulfurization[36] was conducted to convert all the Cys residues back to the native Ala residues. The full-length peptide **8** was thus obtained on a 50 mg scale with an overall yield of 4.5% (Figure 1C). After characterization with reversed-phase high-performance liquid chromatography (RP-HPLC) and electrospray ionization mass spectrometry (ESI-MS), **8** was subjected to urea-gradient dialysis to afford folded K27-linked diUb with good homogeneity on size exclusion chromatography (Figure 1D). To verify that the K27-linked isopeptide bond was installed, we performed MS/MS sequencing on synthetic diUb. The MS/MS sequencing data confirmed the specific formation of the Lys27-linked isopeptide bond with a false discovery rate <1% (Supporting Information, Figure S5). The circular dichroism (CD) spectrum of folded K27-linked diUb (Figure 1E) showed characteristic peaks at 208 and 226 nm similar to the spectrum of monoUb, suggesting that each Ub unit in the synthetic chain retains its globular conformation.

We obtained crystals of K27-linked diUb after extensive crystallization trials, but they were of poor diffraction-quality. To overcome the problem, we turned to a unique capability of total protein synthesis, namely, preparation of D-proteins for quasi-racemic crystallography.[37] This technology involves crystallization of protein mixtures of equal amounts of L- and D-proteins with some minor structural difference, which has the advantage of offering higher success rate of crystallization.[38−49] Thus, D-K27-linked diUb was synthesized using the same synthetic route as described above (Supporting Information). Our synthetic D-protein had two mutations to simplify its

DOI: 10.1021/jacs.6b04031
J. Am. Chem. Soc. 2016, 138, 7429−7435

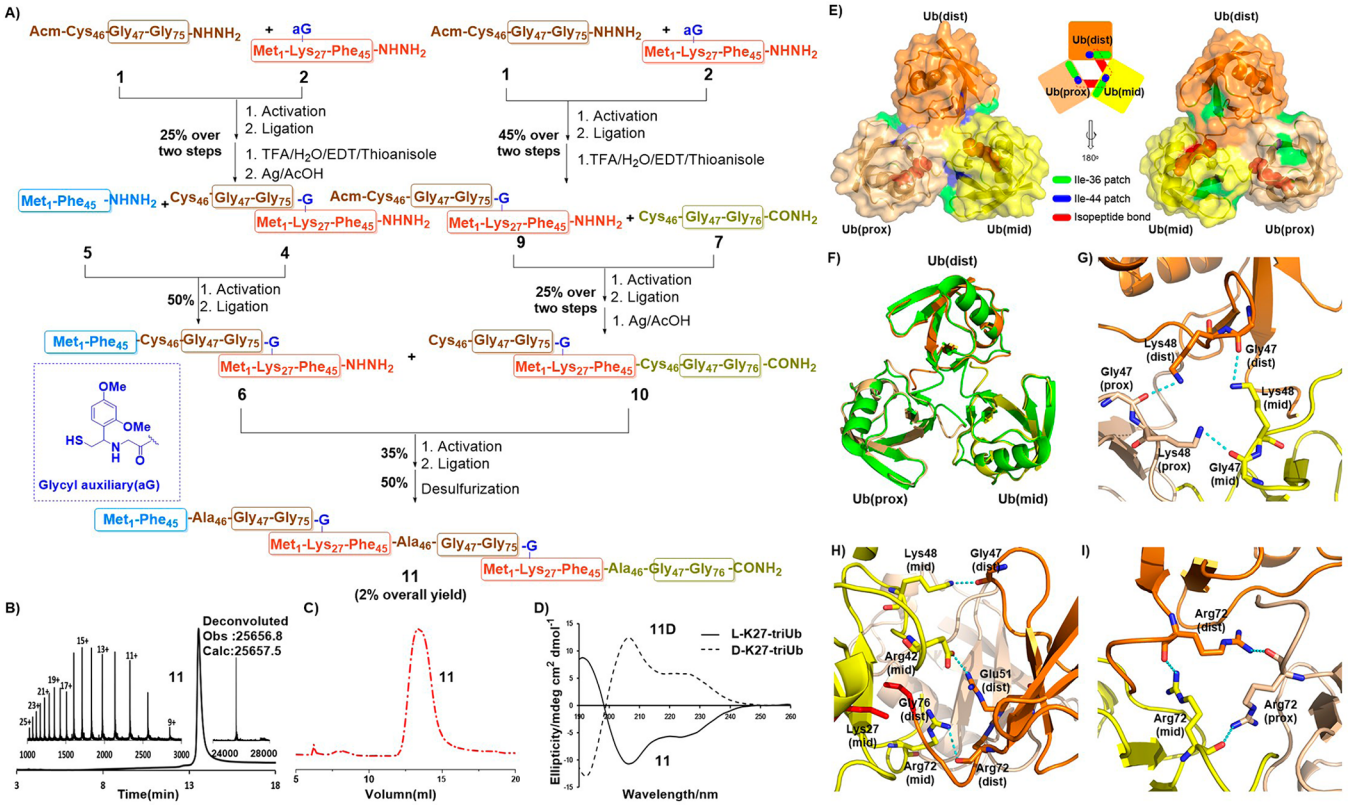

Figure 2. K27-linked triUb. (A) Synthetic route. (B) Analytical HPLC chromatogram (λ = 214 nm) of isolated product **11**. Inset: Observed ESI-MS of the main peak and deconvoluted electrospray ionization mass spectrum of **11** (observed mass = 25 656.8 Da, calculated mass = 25 657.5 Da, average isotopes). (C) Gel filtration chromatography (λ = 280 nm, Superdex 75 column (10/300 GL)) of **11**. (D) Circular dichroism spectra of L- and D-forms (Figure S4) of K27-linked triUb. (E) Schematic drawing of triangle-shaped K27-linked triUb (PDB: 5JBV) (center) and two views of K27-linked triUb crystal structure (left and right), with the distal Ub (orange), the proximal Ub (yellow), the middle Ub (wheat), and the inside isopeptide bonds showed in spheres (red). Ile36 and Ile44 patches are colored in green and blue, respectively. (F) Alignment of monoUb (green) with each Ub units in K27-linked triUb. (G) Top view of K27-linked triUb. The polar interactions (<3.5 Å) between Gly47(dist) and Lys48(mid), Gly47(mid) and Lys48(prox), and Gly47(prox) and Lys48(dist) are connected with cyan dotted lines. (H) Close-up view of the interface between distal Ub and middle Ub in K27-linked triUb. The polar interactions between Arg42(dist) and Glu51(mid), Arg72(dist) and Arg72(mid), and Gly47(dist) and Lys48(mid) are connected with cyan dotted lines, and the isopeptide bonds of Gly76(dist) and Lys27(prox) are drawn in red sticks. (I) Bottom view of K27-linked triUb. The polar interactions between Arg72(prox), Arg72(mid), and Arg72(dist) are connected with cyan dotted lines.

synthesis. First, Met1 was mutated to Nle to avoid Met oxidation. Second, Cys was used to replace glycyl auxiliary to simply the ligation.

Synthetic L- and D-K27-linked diUb's were crystallized as a quasi-racemic protein mixture. Diffraction-quality crystals were obtained with only 50 commercial screening conditions. One of the crystals grown from 0.2 M magnesium acetate tetrahydrate, 0.1 M sodium cacodylate trihydrate, pH 6.5, 20% PEG8000 formed in a monoclinic space group (C2) and diffracted X-rays to 1.6 Å resolution. Its structure was solved by molecular replacement and refined to the final statistics (Supporting Information, Table S2). As shown in Figure 2B, K27-linked diUb (PDB: 5J8P) bears a symmetric compact conformation. Similar conformation was previously reported for K11-,[12] K33-,[16,17] and K48-linked diUb's.[14] The isopeptide linkage between Gly76(dist) and Lys27(prox) cannot be built in the electron density maps due to the indiscernible electron density of Gly76(dist), but both Gly75(dist) and the ε-amino group of Lys27(prox) are clearly built in the electron density map confirming the formation of Lys27 isopeptide linkage (Supporting Information, Figure S6A).

Each Ub of K27-linked diUb retains the conformation of monomeric Ub (PDB: 1UBQ) except for the C-terminals (Figure 1G). The more regular C-terminals of both Ub units are found to participate in the interdomain Ub-Ub contacts (red, Figure 1H,I). Contacts observed in the crystal structure include the following interactions: Glu24(dist)-Arg74(prox), Glu51(dist)-Arg72(prox), Asp52(dist)-Gly75(prox), Glu24-(prox)-Arg74(dist), Glu51(prox)-Arg72(dist), and Asp52-(prox)-Gly75(dist) (Figure 1I). These Ub-Ub contacts are polar interactions and do not involve the classical Ub hydrophobic surfaces (Ile36 and Ile44 patchs). Similar polar Ub-Ub interactions were observed for K11-linked diUb,[12] whereas only hydrophobic patch interactions were found in the compact conformations of K6-, K33-, and K48-linked diUb's.[11,14−16,18] The hydrophobic patches (Ile36 and Ile44) of Lys27-linked diUb are solvent-exposed (blue and green in Figure 1F). These exposed hydrophobic patches may provide handles for the interaction of K27-linked Ub chains with ubiquitin binding domains and DUBs.

Lys27 isopeptide linkage in the crystal structure is entirely buried within acceptor Ub (sphere (red) in Figure 1F, Supporting Information, Figure S6A,B). By comparison, the isopeptide linkages in all the other Ub's are surface-located and solvent-exposed (Figure 1J). Thus, the buried isopeptide linkage is a property unique to K27-linked diUb. This structural

DOI: 10.1021/jacs.6b04031
J. Am. Chem. Soc. 2016, 138, 7429−7435

feature may contribute to the distinctive biological functions of K27-linked Ub's, for instance, that fewer E2's or E3's have been identified for biosynthesis of K27-linked Ub.[23,24] Our finding is consistent with Fushman's NMR experiments,[27] which showed that the Ub-Ub linker via K27 was the least solvent accessible of all polyUb chains.

Total Synthesis and Structure Determination of K27-Linked triUb. The symmetric conformation of K27-linked diUb raises a question as to the structures of longer K27-linked Ub's. Thus, we synthesized and solved the structure of K27-linked triUb. This protein with 228 aa was divided into six peptide segments (namely, **1**, **1**, **2**, **2**, **5**, and **7**) that can be readily prepared by microwave-assisted SPPS (Figure 2A).

Ligation of **1** and **2** and subsequent TFA treatment produced **9**. Removal of the Acm group from **9** resulted in the formation of **4**. In a convergent fashion, **5** and **4** were ligated to generate **6**, while **9** and **7** were ligated to generate **10**. Subsequently **6** and **10** were ligated to generate the full-length peptide. Final desulfurization transformed Cys46 in the three Ub units into Ala46 to generate the native K27-linked triUb **11** on a ten-milligram scale with an overall yield of 2%. Purified triUb **11** was successfully characterized using RP-HPLC and ESI-MS (Figure 2B).

After folding through urea-gradient dialysis, size exclusion chromatography showed that the folded K27-linked triUb eluted as a single peak with good homogeneity (Figure 2C). The CD spectrum of folded K27-linked triUb (Figure 2D) was consistent with that of K27-linked diUb exhibiting double negative peaks at 208 and 226 nm.

We also synthesized the D-form of K27-linked triUb again bearing the Nle1 and Ala76 mutations (Supporting Information). The L- and D-K27-linked triUb's were subjected to quasi-racemic crystallization. Diffraction-quality crystals of K27-linked triUb were obtained from only 50 commercial screening conditions. Crystals grown from 20% (w/v) PEG 3350, 4 mM $CdCl_2$, pH 5.9, 200 mM $Mg(NO_3)_2$ formed in a hexagonal space group (H3) and diffracted X-rays to 2.1 Å resolution. Its structure was solved by molecular replacement and refined to the final statistics (Supporting Information, Table S2). The isopeptide bonds in the crystal structure of K27-linked triUb were again not fully resolved in electron density map, although our MS/MS sequence experiment verified their correct positions (Supporting Information, Figure S5). In contrast to the symmetric compact conformation of K27-linked diUb, K27-linked triUb adopts a triangular conformation possessing a C3 rotation axis (PDB: 5JBV). Each Ub unit would overlap with the neighboring Ub units when rotated ±120 degrees around the C3-axis (Figure 2E).

All the Ub units in K27-linked triUb adopt monoUb conformation (PDB: 1UBQ) except for the C-terminals (Figure 2F). Several polar interactions stabilize the triangular structure. These include three polar interactions on the top between Gly47 and Lys48 of neighboring Ub's, three in the middle between Arg42 and Glu51 of neighboring Ub's, and three at the bottom between Arg72 and Arg72 of neighboring Ub's (Figure 2G–I). Similar to the structure of K27-linked diUb, the Ile36 and Ile44 hydrophobic patches of all Ub units in K27-linked triUb are surface-located and solvent-exposed. Finally, both of the two isopeptide bonds in K27-linked triUb are entirely inner-buried (Figure 2E,H).

Different Activity of K27-Linked diUb and triUb toward OTUD2. The snapshots show that K27-linked di- and triUb observed from the crystal structures adopt different conformations, one being symmetric and the other triangular (Figures 1F and 2E). The two conformations offer distinct binding surfaces, posing a question whether K27-linked di- and triUb may exhibit different activities toward DUBs. Thus, we incubated K27-linked di- and triUb with OTUD2 (ovarian tumor family) that was previously known to cleave K27-linked diUb.[50] Our experiments showed that OTUD2 can hydrolyze both K27-linked di- and triUb (Figure 3A, and Supporting Information, Figure S7A). However, K27-linked triUb is more rapidly hydrolyzed by OTUD2 than K27-linked diUb (Supporting Information, Figure S7A,B). As shown in Figure 3A, K27-linked triUb is fully hydrolyzed by OTUD2 to di- and monoUb within 30 min, whereas only a small portion of K27-linked diUb is hydrolyzed by OTUD2 to monoUb after 30 min.

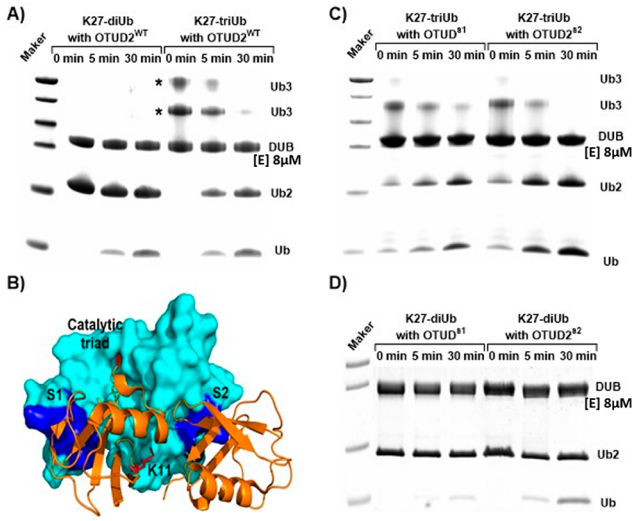

Figure 3. DUB assay of K27-linked Ub's. (A) DUB assay of OTUD2 (residues 132–348) toward K27-linked di- and triUb. Note: K27-linked triUb is labeled with a star in SDS-PAGE. The presence of two extra bands is caused by the heating treatment of the loaded samples. For more details, please see discussion in the Supporting Information. (B) Surface representation of OTU domain of OTUD2 (cyan) bound to K11-linked diUb molecule (orange), with its C terminus reaching to the catalytic triad (red). Ub binding sites S1 and S2 are how in blue. (C,D) DUB assays of OTUD2 mutants with K27-linked di- and triUb. Note: The occurrence of cleaved monoUb and diUb at time point 0 min in panel (C) is due to the imprecise time control. Domain composition of human OTUD2 with different variants, WT OTUD2 ($OTUD2^{WT}$, residues 132–348), S1 site mutant ($OTUD2^{S1}$, residues 132–348, I201Q), and S2 site mutant ($OTUD2^{S2}$, residues 132–348, I292Q, V295Q).

A similar observation was recently reported by Komander et al. for the cleavage of K11-linked triUb and diUb by OTU domain of OTUD2 (confirmed by our experiments as shown in Supporting Information, Figure S7B).[50] Komander's explanation for the activity difference is that the OTU domain of OTUD2 not only contains the previously defined Ub binding site S1, but also an additional Ub binding site S2 that allows preferential binding of K11-linked triUb over diUb (Figure 3B, Supporting Information, Figure S7C,E). However, this theory does not appear to be applicable for K27-linked Ub's, because WT OTUD2 (residues 132–348) and OTUD2 S2 site mutant (residues 132–348, I292Q, V295Q) are found to hydrolyze K27-linked triUb with similar rates (Figure 3C, Supporting Information, Figure S7D,F,G).

DOI: 10.1021/jacs.6b04031
J. Am. Chem. Soc. 2016, 138, 7429–7435

On the other hand, OTUD2 S1 mutant (residues 132−348, I201Q) cannot effectively hydrolyze K27-linked diUb (Figure 3D, Supporting Information, Figure S7D,G), but can still hydrolyze K27-linked triUb (Figure 3C, Supporting Information, Figure S7F,G). This finding cannot be interpreted in the context of the previous mechanism of OTU family DUB, which says that the distal Ub should bind to the S1 site of OTU domain and positions its C-terminal tail in the catalytic site[50] (Supporting Information, Figure S7H). A more plausible explanation is that K27-linked di- and triUb's may have different binding modes with OTUD2, which is consistent with the observation of distinct conformations of K27-linked di- and triUb's from the crystal structures. Further elucidation of the reactivity difference between K27-linked di- and triUb requires structural studies on the enzyme−substrate complexes.

■ CONCLUSION

In summary, we report total chemical synthesis of K27-linked di- and triUb using the hydrazide-based native chemical ligation. Using the technology of quasi-racemic crystallography, we obtained the X-ray structures of K27-linked di- (resolution 1.6 Å) and triUb's (resolution 2.1 Å) for the first time. A key finding is that the isopeptide bond of K27-linked Ub chains is buried in the acceptor Ub and unique when compared with all the other seven Ub chains. Ovarian tumor family de-ubiquitinase 2 (OTUD2) was found to exhibit significantly different activity for K27-linked di- and triUb's. Mutagenesis assays revealed that K27-linked di- and triUb's may have different binding modes with OTUD2. Our work highlights the usefulness of chemical protein synthesis[51] for the access to Ub chains with good quantity and quality for biochemical and structural studies. K27-linked triUb represents the so-far largest chemically synthesized protein (228 aa) that has been crystallized to afford a high-resolution X-ray diffraction structure.

■ EXPERIMENTAL SECTION

Detailed experimental procedures for the synthesis of compounds, peptides, and proteins, their characterization data, and methods of cloning of de-ubiquitinase OTUD2 are given in the Supporting Information.

General Fmoc Solid-Phase Peptide Synthesis. All the peptides were synthesized using standard Fmoc SPPS protocols under microwave conditions (CEM Liberty Blue) starting from Rink Amide MBHA PS resin or Fmoc-hydrazine 2-chlorotrityl chloride PS resin.[52] Each coupling cycle includes Fmoc deprotection using 20% piperidine in DMF with 0.1 M Oxyma (1 min at 90 °C) and amino acid coupling using 4-fold excess of 0.2 M Fmoc-protected amino acid in DMF, 1.0 M DIC in DMF, and 1.0 M Oxyma in DMF (10 min at 50 °C for His and Cys, 75 °C for other residues).[33] After the completion of SPPS, the resulting peptide-resin was transferred into customized sand core funnel and treated with the cleavage cocktail (87% trifluoroacetic acid, 5% water, 5% thioanisole, 3% 1,2-ethanedithiol) for 3 h at room temperature. Crude peptides were precipitated with cold diethyl ether and purified by semi-preparative RP-HPLC. Purified peptides were characterized by analytical RP-HPLC (20−60% acetonitrile in water over 30 min) with an analytical C18 column (Grace) and ESI-MS.

General Protocol of Hydrazide-Based Native Chemical Ligation. The hydrazide peptide (1 μmol, 1 equiv) was dissolved in 1 mL of ligation buffer (6 M Gn-HCl, 200 mM NaH_2PO_4, pH 3.0) precooled in an ice bath (−10 °C). Then 10 μL of 1 M $NaNO_2$ (10 μmol, 10 equiv) was added dropwise, and the reaction was incubated for 30 min at −10 °C to fully convert the hydrazide to the acyl azide. Next MPAA (6.8 mg, 40 μmol, 40 equiv) was added, and the pH was adjusted to 5.0 for 5 min to generate the thioester peptide. Finally, the N-terminal Cys peptide (1 μmol, 1 equiv) was added, and the pH was adjusted to 6.5 to initiate the ligation. The reaction was monitored by analytical RP-HPLC.[29−31]

Protein Crystal Generation. The protein solution comprised 1.5 mg/mL of each K27-linked di- and triUb enantiomer (3 mg/mL total protein) in 10 mM Tris buffer (pH 7.4). Crystals of racemic mixture of K27-linked di- and triUb were grown in sitting drops at 293 K. Crystals grew overnight and reached maximum size after 3 days. The resulting crystals were soaked in oil for cryo-protection. Diffraction data were collected at BL17U line station at the Shanghai Synchrotron Radiation Facility (SSRF).

Data Collection and Structure Determination. X-ray data were collected at the SSRF beamline BL17U1 using an ADSC CCD area detector. Data were processed using the HKL-2000 package[53] or XDS.[54] The data collection statistics are summarized in Supporting Information, Table S2. All calculations were performed with programs from the CCP4 suite,[55] unless explicitly specified otherwise. The structures were determined by molecular replacement (MR) method with the ubiquitin (PDB ID: 1UBQ) as search model using PHASER.[56] The manual model building was performed in COOT.[57,58] The structure refinement was done using PHENIX[59,60] after excluding 5% of the data for the R-free calculation.

De-ubiquitinase Assays in Vitro. For DUB assays with OTUD2 mutants produced in *E. coli*, 8 μM OTUD2 mutants were mixed with 20 μM K27-linked Ub chains in 40 μL of reaction mixture (Ub's concentrations are re-adjusted frequently.[50]). All the DUB essays were conducted in DUB buffer consisting of 150 mM NaCl, 20 mM Tris, pH 7.5, and 1 mM DTT. Reactions were stopped by mixing 10 μL of reaction buffer and 4 μL of 4× loading sample buffer (containing 400 mM DTT) at 0, 5, 30, and 50 min at 37 °C, and boiled at 95 °C for 2 min. Ub cleavage was detected by staining with Coomassie brilliant blue.

■ ASSOCIATED CONTENT

Supporting Information

The Supporting Information is available free of charge on the ACS Publications website at DOI: 10.1021/jacs.6b04031.

Experimental details and compound characterizations (PDF)

■ AUTHOR INFORMATION

Corresponding Author

*lliu@mail.tsinghua.edu.cn

Author Contributions

#M.P., S.G., and Y.Z. contributed equally.

Notes

The authors declare no competing financial interest.

■ ACKNOWLEDGMENTS

We thank the protein chemistry facility at the Center for Biomedical Analysis of Tsinghua University for sample analysis. This study was supported by the National Basic Research

DOI: 10.1021/jacs.6b04031
J. Am. Chem. Soc. 2016, 138, 7429−7435

Program of China (973 program, No. 2013CB932800) and NSFC (Nos. 21532004 and 21225207).

REFERENCES

(1) Hershko, A.; Ciechanover, A. *Annu. Rev. Biochem.* **1998**, *67*, 425.
(2) Komander, D.; Rape, M. *Annu. Rev. Biochem.* **2012**, *81*, 203.
(3) Ikeda, F.; Dikic, I. *EMBO Rep.* **2008**, *9*, 536.
(4) Schulman, B. A.; Harper, J. W. *Nat. Rev. Mol. Cell Biol.* **2009**, *10*, 319.
(5) Ye, Y.; Rape, M. *Nat. Rev. Mol. Cell Biol.* **2009**, *10*, 755.
(6) Deshaies, R. J.; Joazeiro, C. *Annu. Rev. Biochem.* **2009**, *78*, 399.
(7) Kulathu, Y.; Komander, D. *Nat. Rev. Mol. Cell Biol.* **2012**, *13*, 508.
(8) Hospenthal, M. K.; Freund, S. M.; Komander, D. *Nat. Struct. Mol. Biol.* **2013**, *20*, 555.
(9) Komander, D. *Biochem. Soc. Trans.* **2009**, *37*, 937.
(10) Meyer, H. J.; Rape, M. *Cell* **2014**, *157*, 910.
(11) Virdee, S.; Ye, Y.; Nguyen, D. P.; Komander, D.; Chin, J. W. *Nat. Chem. Biol.* **2010**, *6*, 750.
(12) Bremm, A.; Freund, S. M.; Komander, D. *Nat. Struct. Mol. Biol.* **2010**, *17*, 939.
(13) Castañeda, C. A.; Kashyap, T. R.; Nakasone, M. A.; Krueger, S.; Fushman, D. *Structure* **2013**, *21*, 1168.
(14) Cook, W. J.; Jeffrey, L. C.; Carson, M.; Chen, Z.; Pickart, C. M. *J. Biol. Chem.* **1992**, *267*, 16467.
(15) Komander, D.; Reyes-Turcu, F.; Licchesi, J. D.; Odenwaelder, P.; Wilkinson, K. D.; Barford, D. *EMBO Rep.* **2009**, *10*, 466.
(16) Michel, M. A.; Elliott, P. R.; Swatek, K. N.; Simicek, M.; Pruneda, J. N.; Wagstaff, J. L.; Freund, S. M.; Komander, D. *Mol. Cell* **2015**, *58*, 95.
(17) Kristariyanto, Y. A.; Choi, S. Y.; Rehman, S. A.; Ritorto, M. S.; Campbell, D. G.; Morrice, N. A.; Toth, R.; Kulathu, Y. *Biochem. J.* **2015**, *467*, 345.
(18) Kristariyanto, Y. A.; Abdul Rehman, S. A.; Campbell, D. G.; Morrice, N. A.; Johnson, C.; Toth, R.; Kulathu, Y. *Mol. Cell* **2015**, *58*, 83.
(19) Ikeda, H.; Kerppola, T. K. *Mol. Biol. Cell* **2008**, *19*, 4588.
(20) Geisler, S.; Holmström, K. M.; Skujat, D.; Fiesel, F. C.; Rothfuss, O. C.; Kahle, P. J.; Springer, W. *Nat. Cell Biol.* **2010**, *12*, 119.
(21) Liu, J.; Han, C.; Xie, B.; Wu, Y.; Liu, S.; Chen, K.; Xia, M.; Zhang, Y.; Song, L.; Li, Z.; Zhang, T.; Ma, F.; Wang, Q.; Wang, J.; Deng, K.; Zhuang, Y.; Wu, X.; Yu, Y.; Xu, T.; Cao, X. *Nat. Immunol.* **2014**, *15*, 612.
(22) Gatti, M.; Pinato, S.; Maiolica, A.; Rocchio, F.; Prato, M. G.; Aebersold, R.; Penengo, L. *Cell Rep.* **2015**, *10*, 226.
(23) Faggiano, S.; Alfano, C.; Pastore, A. *Anal. Biochem.* **2016**, *492*, 82.
(24) Alfano, C.; Faggiano, S.; Pastore, A. *Trends Biochem. Sci.* **2016**, *41*, 371.
(25) Castañeda, C.; Liu, J.; Chaturvedi, A.; Nowicka, U.; Cropp, T. A.; Fushman, D. *J. Am. Chem. Soc.* **2011**, *133*, 17855.
(26) Castañeda, C. A.; Chaturvedi, A.; Camara, C. M.; Curtis, J. E.; Krueger, S.; Fushman, D. *Phys. Chem. Chem. Phys.* **2016**, *18*, 5771.
(27) Castañeda, C. A.; Dixon, E. K.; Walker, O.; Chaturvedi, A.; Nakasone, M. A.; Curtis, J. E.; Reed, M. R.; Krueger, S.; Cropp, T. A.; Fushman, D. *Structure* **2016**, *24*, 423.
(28) (a) Dawson, P. E.; Muir, T. W.; Clark-Lewis, I.; Kent, S. B. H. *Science* **1994**, *266*, 776. (b) Kent, S. B. H. *Chem. Soc. Rev.* **2009**, *38*, 338.
(29) (a) Fang, G. M.; Li, Y. M.; Shen, F.; Huang, Y. C.; Li, J. B.; Lin, Y.; Cui, H. K.; Liu, L. *Angew. Chem., Int. Ed.* **2011**, *50*, 7645. (b) Fang, G.-M.; Wang, J.-X.; Liu, L. *Angew. Chem., Int. Ed.* **2012**, *51*, 10347–10350.
(30) Zheng, J. S.; Tang, S.; Qi, Y. K.; Wang, Z. P.; Liu, L. *Nat. Protoc.* **2013**, *8*, 2483.
(31) (a) Zheng, J. S.; Tang, S.; Huang, Y. C.; Liu, L. *Acc. Chem. Res.* **2013**, *46*, 2475. (b) Huang, Y.; Liu, L. *Sci. China: Chem.* **2015**, *58*, 1779. (c) Huang, Y.-C.; Fang, G.-M.; Liu, L. *Natl. Sci. Rev.* **2016**, *3*, 107.
(32) Pedersen, S.; Tofteng, P.; Malik, L.; Jensen, K. *Chem. Soc. Rev.* **2012**, *41*, 1826.
(33) Collins, J.; Porter, K.; Singh, S.; Vanier, G. *Org. Lett.* **2014**, *16*, 940.
(34) Macmillan, D.; Anderson, D. *Org. Lett.* **2004**, *6*, 4659.
(35) Yang, R.; Bi, X.; Li, F.; Cao, Y.; Liu, C. F. *Chem. Commun.* **2014**, *50*, 7971.
(36) Wan, Q.; Danishefsky, S. J. *Angew. Chem., Int. Ed.* **2007**, *46*, 9248.
(37) Yeates, T.; Kent, S. B. H. *Annu. Rev. Biophys.* **2012**, *41*, 41.
(38) Toniolo, C.; Peggion, C.; Crisma, M.; Formaggio, F.; Shui, X.; Eggleston, D. S. *Nat. Struct. Biol.* **1994**, *1*, 908.
(39) Wukovitz, S. W.; Yeates, T. O. *Nat. Struct. Biol.* **1995**, *2*, 1062.
(40) Pentelute, B. L.; Gates, Z. P.; Tereshko, V.; Dashnau, J. L.; Vanderkooi, J. M.; Kossiakoff, A. A.; Kent, S. B. H. *J. Am. Chem. Soc.* **2008**, *130*, 9695.
(41) Mandal, K.; Pentelute, B. L.; Tereshko, V.; Kossiakoff, A. A.; Kent, S. B. H. *J. Am. Chem. Soc.* **2009**, *131*, 1362.
(42) Mandal, K.; Uppalapati, M.; Ault-Riché, D.; Kenney, J.; Lowitz, J.; Sidhu, S. S.; Kent, S. B. H. *Proc. Natl. Acad. Sci. U. S. A.* **2012**, *109*, 14779.
(43) Mandal, K.; Pentelute, B. L.; Bang, D.; Gates, Z. P.; Torbeev, V. Y.; Kent, S. B. H. *Angew. Chem., Int. Ed.* **2012**, *51*, 1481.
(44) Avital-Shmilovici, M.; Mandal, K.; Gates, Z. P.; Phillips, N. B.; Weiss, M. A.; Kent, S. B. H. *J. Am. Chem. Soc.* **2013**, *135*, 3173.
(45) Okamoto, R.; Mandal, K.; Sawaya, M. R.; Kajihara, Y.; Yeates, T. O.; Kent, S. B. H. *Angew. Chem.* **2014**, *53*, 5294.
(46) Wang, C. K.; King, G. J.; Northfield, S. E.; Ojeda, P. G.; Craik, D. J. *Angew. Chem., Int. Ed.* **2014**, *53*, 11236.
(47) Hayouka, Z.; Thomas, N. C.; Mortenson, D. E.; Satyshur, K. A.; Weisblum, B.; Forest, K. T.; Gellman, S. H. *J. Am. Chem. Soc.* **2015**, *137*, 11884.
(48) Mortenson, D. E.; Steinkruger, J. D.; Kreitler, D. F.; Perroni, D. V.; Sorenson, G. P.; Huang, L.; Mittal, R.; Yun, H. G.; Travis, B. R.; Mahanthappa, M. K.; et al. *Proc. Natl. Acad. Sci. U. S. A.* **2015**, *112*, 13144.
(49) Bunker, R. D.; Mandal, K.; Bashiri, G.; Chaston, J. J.; Pentelute, B. L.; Lott, J. S.; Kent, S. B. H.; Baker, E. N. *Proc. Natl. Acad. Sci. U. S. A.* **2015**, *112*, 4310.
(50) Mevissen, T. E.; Hospenthal, M. K.; Geurink, P. P.; Elliott, P. R.; Akutsu, M.; Arnaudo, N.; Ekkebus, R.; Kulathu, Y.; Wauer, T.; El Oualid, F.; Freund, S. M.; Ovaa, H.; Komander, D. *Cell* **2013**, *154*, 169.
(51) Previous examples for total synthesis of ubiquitins: (a) Kumar, K. S.; Spasser, L.; Erlich, L. A.; Bavikar, S. N.; Brik, A. *Angew. Chem., Int. Ed.* **2010**, *49*, 9126. (b) El Oualid, F.; Merkx, R.; Ekkebus, R.; Hameed, D. S.; Smit, J. J.; de Jong, A.; Hilkmann, H.; Sixma, T. K.; Ovaa, H. *Angew. Chem., Int. Ed.* **2010**, *49*, 10149. (c) Kumar, K. S.; Bavikar, S. N.; Spasser, L.; Moyal, T.; Ohayon, S.; Brik, A. *Angew. Chem., Int. Ed.* **2011**, *50*, 6137. (d) Trang, V. H.; Valkevich, E. M.; Minami, S.; Chen, Y. C.; Ge, Y.; Strieter, E. R. *Angew. Chem., Int. Ed.* **2012**, *51*, 13085. (e) Valkevich, E. M.; Guenette, R. G.; Sanchez, N. A.; Chen, Y. C.; Ge, Y.; Strieter, E. R. *J. Am. Chem. Soc.* **2012**, *134*, 6916. (f) Hemantha, H. P.; Bavikar, S. N.; Herman-Bachinsky, Y.; Haj-Yahya, N.; Bondalapati, S.; Ciechanover, A.; Brik, A. *J. Am. Chem. Soc.* **2014**, *136*, 2665.
(52) Huang, Y. C.; Chen, C. C.; Li, S. J.; Gao, S.; Shi, J.; Li, Y. M. *Tetrahedron* **2014**, *70*, 2951.
(53) Otwinowski, Z.; Minor, W. *Methods Enzymol.* **1997**, *276*, 307.
(54) Kabsch, W. *J. Appl. Crystallogr.* **1993**, *26*, 795.
(55) Bailey, S. *Acta Crystallogr., Sect. D: Biol. Crystallogr.* **1994**, *50*, 760.
(56) McCoy, A. J.; Grosse-Kunstleve, R. W.; Adams, P. D.; Winn, M. D.; Storoni, L. C.; Read, R. J. *J. Appl. Crystallogr.* **2007**, *40*, 658.
(57) Emsley, P.; Lohkamp, B.; Scott, W. G.; Cowtan, K. *Acta Crystallogr., Sect. D: Biol. Crystallogr.* **2010**, *66*, 486.
(58) Emsley, P.; Cowtan, K. *Acta Crystallogr., Sect. D: Biol. Crystallogr.* **2004**, *60*, 2126.

DOI: 10.1021/jacs.6b04031
J. Am. Chem. Soc. 2016, 138, 7429–7435

(59) Adams, P. D.; Afonine, P. V.; Bunkóczi, G.; Chen, V. B.; Davis, I. W.; Echols, N.; Headd, J. J.; Hung, L. W.; Kapral, G. J.; Grosse-Kunstleve, R. W.; McCoy, A. J.; Moriarty, N. W.; Oeffner, R.; Read, R. J.; Richardson, D. C.; Richardson, J. S.; Terwilliger, T. C.; Zwart, P. H. *Acta Crystallogr., Sect. D: Biol. Crystallogr.* **2010**, *66*, 213.
(60) Adams, P. D.; Grosse-Kunstleve, R. W.; Hung, L. W.; Ioerger, T. R.; McCoy, A. J.; Moriarty, N. W.; Read, R. J.; Sacchettini, J. C.; Sauter, N. K.; Terwilliger, T. C. *Acta Crystallogr., Sect. D: Biol. Crystallogr.* **2002**, *58*, 1948.

DOI: 10.1021/jacs.6b04031
J. Am. Chem. Soc. 2016, 138, 7429−7435